Developing a Mobile Lower Limb Robotic Exoskeleton for Gait Rehabilitation

Zhao Guo
State Key Laboratory of Mechanism System and Vibration, Institute of Robotics, Shanghai Jiao Tong University, Shanghai 200240, China;
Department of Biomedical Engineering, National University of Singapore, Singapore 117575, Singapore
e-mail: guozhao@sjtu.edu.cn

Haoyong Yu
Department of Biomedical Engineering, National University of Singapore, Singapore 117575, Singapore
e-mail: bieyhy@nus.edu.sg

Yue H. Yin[1]
State Key Laboratory of Mechanism System and Vibration, Institute of Robotics, Shanghai Jiao Tong University, Shanghai 200240, China
e-mail: yhyin@sjtu.edu.cn

A new compact mobile lower limb robotic exoskeleton (MLLRE) has been developed for gait rehabilitation for neurologically impaired patients. This robotic exoskeleton is composed of two exoskeletal orthoses, an active body weight support (BWS) system attached to a motorized mobile base, allowing over-ground walking. The exoskeletal orthosis is optimized to implement the extension and flexion of human hip and knee joints in the sagittal plane. The motor-driven BWS system can actively unload human body weight and track the vertical displacement of the center of mass (COM). This system is compact and easy for therapist to help patient with different weight (up to 100 kg) and height (150–190 cm). Experiments were conducted to evaluate the performance of the robot with a healthy subject. The results show that MLLRE is a useful device for patient to achieve normal over-ground gait patterns. [DOI: 10.1115/1.4026900]

1 Introduction

Robotic exoskeletons have attracted much attention in the rehabilitation community for patients suffering from neurological disorders, such as traumatic brain injury, spinal cord injury, stroke, and cerebral palsy [1,2]. These robotic systems provide active and repetitive controlled movements to help patients recover mobility, relieving the physical therapists from the onerous task of manual assistance and training. Since the first active exoskeleton appeared in the late 1960s, many novel robotic exoskeletons have been developed for the assistance and rehabilitation of human lower limb [3]. Primarily, these devices are differentiated by means of the function and as such, they can be classified into three categories: portable lower limb exoskeleton, treadmill-based exoskeleton, and over-ground rehabilitation robot.

The portable lower limb exoskeleton is a new type of active exoskeleton suit, aiming to assist paraplegics standing and walking over-ground. These exoskeletons are designed to be lightweight, simple, and powerful for users. In recent years, several systems, such as eLEGS [4], Rewark [5], and Indego [6], have been developed for independent walking. However, the operating time of this type of exoskeleton is limited by the battery and a set of crutches is employed to maintain body balance and protect user from falling. In order to do continuous gait training, another kind of rehabilitation robot, the treadmill-based exoskeleton, which consists of powered leg orthosis and body weight support (BWS) system on a moving treadmill, is designed for neurological patients. This training has shown significant improvements in gait recovery by reducing the gravitational force on human legs [7]. The exoskeleton, LOKOMAT, has been successfully commercialized and utilized in clinics [8]. Other treadmill-based exoskeletons, LOPES [9], ReoAmbulator (Motorika, USA), and ALEX [10] have also been developed.

The third type of exoskeleton is the over-ground rehabilitation robot which incorporated a mobile platform into the robotic system, for example, WalkTrainer [11] and NaTUre-gaits [12]. Compared to the treadmill-restricted training, the most important function of this type of exoskeleton is the ability of over-ground walking, allowing patients to have a realistic experience and increasing the independence of gait training. However, these existing mobile robotic systems include a complex mechanical structure to implement the function of walking and BWS. It is desirable to develop a safe, compact and over-ground exoskeleton for patients with lower limb motor impairments. A robotic walker, called KineAssist [13], which consists of a custom designed torso and a pelvis harness attached to a mobile base, can fulfill different types of walking modes. However this robot lacks of actuated orthosis to assist the human leg.

This article introduces a novel compact mobile lower limb robotic exoskeleton (MLLRE) developed for gait training. This exoskeleton consists of two wearable robotic orthoses to assist patient walking, an active BWS system to unload the body weight and a mobile base to move over-ground.

2 Design Objectives and Requirements

2.1 Design Objectives. The goal of this project is to develop a mobile device for gait rehabilitation. The main component is the robotic orthosis designed to realize two degrees of freedom (DOFs), the extension/flexion of the hip and knee joints in the sagittal plane. The working range of each DOF should be large enough to meet the demand of human walking. An active BWS system combined with a mobile base is developed to support body weight and implement over-ground walking. In addition, the exoskeleton should be realized with several layers of safety checks. To accommodate most adult (50–100 kg), the width between two orthoses should be adjusted.

2.2 Biomechanical Requirements. From the perspective of kinematics and functionality of each joint during walking, the biomechanical requirements, including the angle, torque and power, are essential for powered exoskeleton design. Clinical Gait Analysis (CGA) data on hip, knee flexion/extension in a normal, healthy subject (75 kg) walking at 1.3 m/s, was given by Ref. [14]. Generally, the walking knee flexion is limited to approximately 70 deg, while the knee has a significant flexibility (up to 160 deg). The walking hip extension/flexion ranges from −20 deg to 25 deg. With respect to the joint torque, the required knee torque has both positive and negative components. The peak knee torque is approximately $60\text{N}\cdot\text{m}$ which occurs at the early stance during extension. The hip torque ranges from $-80\text{to}60\text{N}\cdot\text{m}$. An average mechanical power between 100 W and 150 W is required to move the subject. During normal walking, the center of mass (COM) moves in a regular sinusoidal pattern in the vertical direction. The amplitude in the normal adult male is approximately 5 cm [15].

[1]Corresponding author.

Manuscript received August 8, 2013; final manuscript received February 17, 2014; published online August 19, 2014. Assoc. Editor: Venketesh N. Dubey.

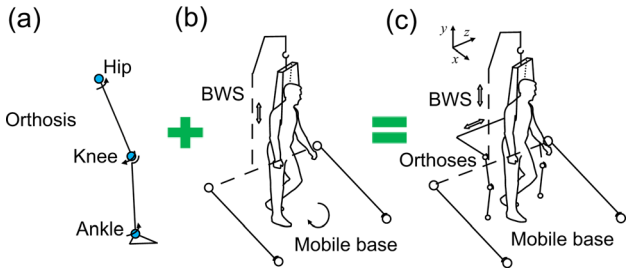

Fig. 1 Schematic graph of the MLLRE: (*a*) robotic gait orthosis, (*b*) mobile base combining with BWS system, and (*c*) the integrated structure of the robotic system

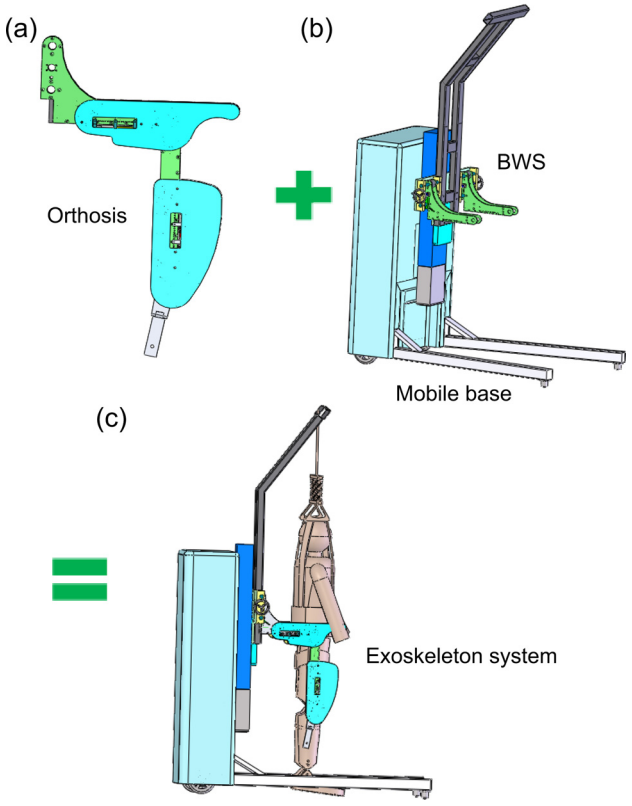

Fig. 2 CAD models of the MLLRE: (*a*) robotic gait orthosis, (*b*) mobile base incorporating with BWS system, and (*c*) the integrated robotic system

3 MLLRE Design

Figure 1 shows the schematic graph of the MLLRE. The computer-aided design (CAD) models of the proposed compact MLLRE were implemented, as shown in Fig. 2.

3.1 Robotic Gait Orthosis. The exoskeletal orthosis consists of two active joints for the extension/flexion of hip and knee joints, as well as a passive spring lifter to support ankle dorsiflexion in the sagittal plane. In the existing motor-driven exoskeleton design, four-bar linkage is normally applied to create an active orthosis. The schematic structures of the orthoses shown in Figs. 3(*a*) and 3(*b*) are utilized in LOKOMAT [16] and ALEX [10], respectively. In these two structures, the connecting rod is set as an active linkage between the thigh and calf segments. Different from this arrangement, we introduced an offset slider-crank mechanism into our robot design (Fig. 3(*c*)). The active linkage, driven by a ball screw transmission, is located in the thigh segment. The

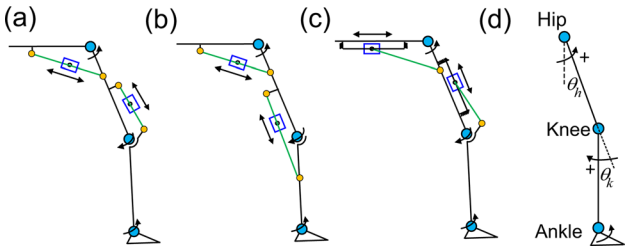

Fig. 3 Schematic graph of three different robotic orthosis: four-bar linkage mechanism in LOKOMAT (*a*), in ALEX (*b*), offset slider-crank mechanism in our MLLRE (*c*), and (*d*) the definition of knee and hip joint angles with the positive direction indicated

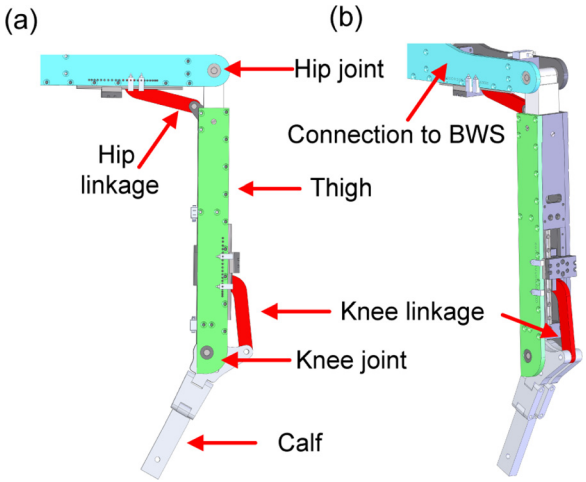

Fig. 4 Robotic orthosis: (*a*) the side view and (*b*) the 45 deg view of the CAD model

connecting rod is replaced by a lightweight passive linkage, which makes the whole orthosis simple and compact. Fig. 3(*d*) shows the definition of the joint angle. Hip angle (θ_h) is the deviation from the vertical axis. Knee angle (θ_k) is the deviation from the thigh. The initial state of the orthosis is perpendicular to the horizontal ground. The CAD model of the orthosis is illustrated in Fig. 4.

3.1.1 Motion Analysis. As shown in Fig. 5(*a*), the offset slider-crank mechanism in the robotic orthosis is schematically represented as constitution of four members: frame, crank, connecting rod, and the slider. The hip and knee angles are derived from kinematics as the function of the slider displacement x. According to the geometry of the offset slider-crank mechanism, the position equations are given by

$$\begin{cases} l_1 \sin\theta - e = l_2 \sin\varphi \\ l_3 = l_1 \cos\theta + l_2 \cos\varphi \end{cases} \tag{1}$$

Knowing the design parameters (l_1, l_2, l_3, and e), the crank angle and the connecting rod angle in the slider-crank mechanism can be derived. The crank angle is written as

$$\theta = \arctan\left(\frac{l_2 \sin\varphi + e}{l_3 - l_2 \cos\varphi}\right) \tag{2}$$

where

$$\varphi = \arccos\left(\frac{l_3^2 + e^2 + l_2^2 - l_1^2}{2l_2\sqrt{l_3^2 + e^2}}\right) - \arctan\left(\frac{e}{l_3}\right) \tag{3}$$

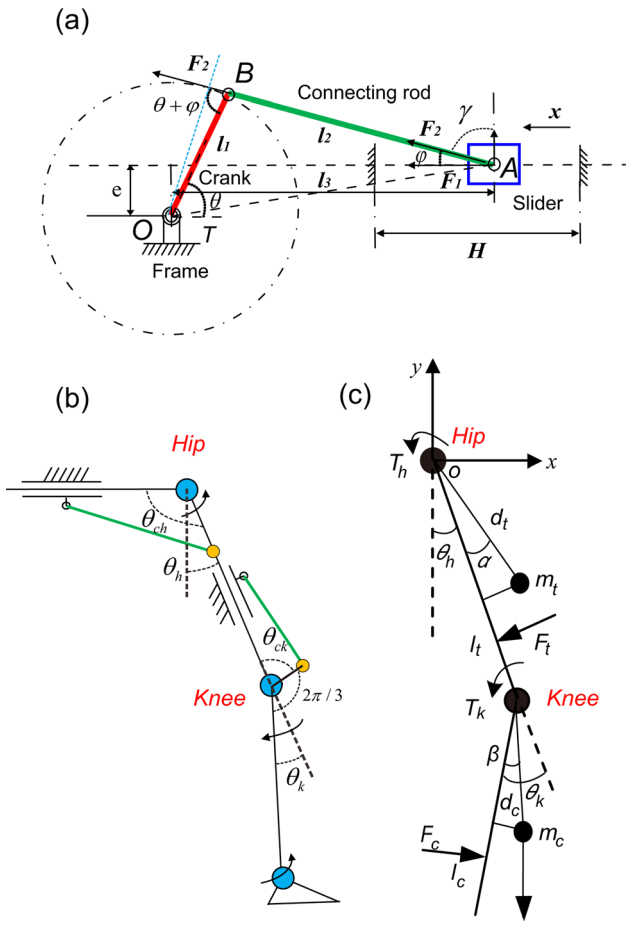

Fig. 5 (*a*) A labeled schematic of the offset slider-crank mechanism, x is the slider displacement, l_1 is the crank length, l_2 is the connecting rod length, l_3 is the length from the slider center to the rotation center along the x direction, e is the eccentricity, and H is the stroke of the slider. θ, ϕ, and γ are the crank angle, connecting rod angle, and transmission angle, respectively. F_1 is the active force produced by the ball screw and F_2 is the force acted on the connecting rod. (*b*) Relationship between the crank angle and the joint angle, we define θ_{ch}, θ_{ck} as the crank angle in the hip and knee, respectively. (*c*) The mechanical diagram of the robotic orthosis. d_t is the distance between the hip joint and the mass center of the thigh, d_c is the distance between the knee joint and the mass center of the calf, α and β are eccentric angles of the mass center away from the centerline of the thigh and calf, T_h and T_k are the joint required torques, F_t and F_c are the interaction forces, l_t and l_c are the interaction force arms, m_t is the mass of the thigh(including the motor), and m_c is the mass of the calf.

and the transmission angle

$$\gamma = ar\cos((l_1 \sin\theta - e)/l_2) \tag{4}$$

The slider displacement x is determined by

$$x = l_{3r} - l_3 \tag{5}$$

where l_{3r} is the initial length of l_3. When the orthosis is in rest position, each joint angle satisfies $\theta_h = 0$, $\theta_k = 0$. The joint angle is related to the crank angle, and we design

$$\begin{cases} \theta_h = \theta_{ch} - \pi/3 \\ \theta_k = \theta_{ck} - \pi/3 \end{cases} \tag{6}$$

3.1.2 Dynamic Analysis. The mechanical schematic diagram of the robotic orthosis is shown in Fig. 5(*c*). Compared to the weight of the thigh and calf, the passive linkage is small and its inertia is neglected. The dynamic model is developed based on the Lagrangian formulation,

$$\begin{cases} L = K - P \\ T'_h = \dfrac{d}{dt}\dfrac{\partial L_h}{\partial \dot{\theta}_h} - \dfrac{\partial L_h}{\partial \dot{\theta}_h} \\ T'_k = \dfrac{d}{dt}\dfrac{\partial L_k}{\partial \dot{\theta}_k} - \dfrac{\partial L_k}{\partial \dot{\theta}_k} \end{cases} \tag{7}$$

where $K = K_h + K_k$, $P = P_h + P_k$. Substituting the kinematic data from CGA, the required torque at the hip and knee with empty load can be obtained from these equations [17],

$$\begin{bmatrix} T_h \\ T_k \end{bmatrix} = \begin{bmatrix} D_{hh} & D_{hk} \\ D_{kh} & D_{kk} \end{bmatrix} \begin{bmatrix} \ddot{\theta}_h \\ \ddot{\theta}_k \end{bmatrix} + \begin{bmatrix} D_{hhh} & D_{hkk} \\ D_{khh} & D_{kkk} \end{bmatrix} \begin{bmatrix} \dot{\theta}_h^2 \\ \dot{\theta}_k^2 \end{bmatrix} + \begin{bmatrix} D_{hhk} & D_{hkh} \\ D_{khk} & D_{kkh} \end{bmatrix} \begin{bmatrix} \dot{\theta}_h \dot{\theta}_k \\ \dot{\theta}_k \dot{\theta}_h \end{bmatrix} + \begin{bmatrix} D_h \\ D_k \end{bmatrix} + \begin{bmatrix} D_{F_t} \\ D_{F_c} \end{bmatrix} \tag{8}$$

The required joint torque includes the dynamic requirement of the robot with empty load and the human torque during gait cycle. Since the walking speed is slow, the mass of the ball screw is small, its inertia is neglected. We derive the required motor torque T_m according to the offset slider-crank transmission mechanism

$$T_m = \frac{p}{2\pi\eta l_1} \frac{\cos\varphi}{\sin(\theta+\varphi)} T \tag{9}$$

where p is the screw lead and η is the transmission efficiency. T is the required joint torque.

3.1.3 Geometrical Optimization. The transmission angle is an indicator to describe the transmission performance of the slider-crank mechanism. With large transmission angle, this mechanism can obtain better transmission performance and higher efficiency. In this optimization, the minimum transmission angle (when $\sin\theta = 1$) was considered as the subjective function. The design variables, including l_1, l_2, l_3, and e, are restricted in a range due to physical limitations. The optimization design problem can be defined as

$$\max \gamma_{min} = \arccos((l_1 - e)/l_2)$$

subject to

$$\begin{cases} 2\pi/9 \le \gamma_{min} \le \pi/2 \\ 6\,\text{mm} \le e \le 40\,\text{mm} \\ 55\,\text{mm} \le l_1 \le 65\,\text{mm} \\ 90\,\text{mm} \le l_2 \le 120\,\text{mm} \end{cases} \tag{10}$$

Because of the limited length of the trunk, the stroke of the slider in the hip and knee is selected as $H_h = 92$ mm, $H_k = 92$ mm, respectively. The optimized solution was found using a constrained nonlinear optimization method with Matlab toolbox. A set of parameters that satisfies the constraints is shown in Table 1. The minimum transmission angles for the hip and knee are 61.8 deg and 73.8 deg. The slider displacement x is in the range of –29 $\le x_h \le$ 63 mm, $0 \le x_k \le$ 92 mm. The range of motion (ROM) of each joint is calculated as –30 deg $\le \theta_h \le$ 65 deg, 0 deg $\le \theta_k \le$ 120 deg. This range can meet the motion demand of normal gait. Other designed parameters are as follows: $d_t = 0.27$ m,

Table 1 The optimized results on the hip and knee joints

Parameters	Hip joint	Knee joint
l_{3r} (mm)	129	136
e (mm)	9	30
l_1 (mm)	60	60
l_2 (mm)	108	108
x (mm)	−29 to 63	0–92
θ (deg)	−30 to 65	0–120

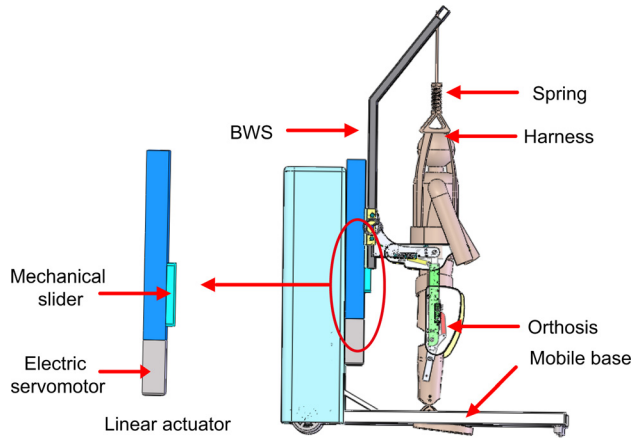

Fig. 6 CAD models of the BWS system

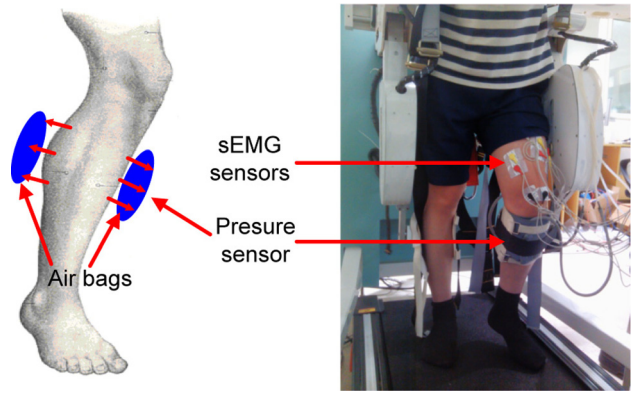

Fig. 7 Pressure and sEMG sensors

$d_c = 0.06$ m, $l_t = 0.2$ m, $l_c = 0.18$ m, $m_t = 4.3$ kg, $m_c = 0.51$ kg, $\alpha = 8.5$ deg, and $\beta = 14.5$ deg.

3.2 Active BWS System. BWS system is another essential part of the treadmill-based or over-ground rehabilitation robot for patients with neurological impairments. Specifically, the weak muscular condition of patients requires an unloading of their weights. BWS is utilized to reduce the load that patients need to overcome during training. This device also guarantees the safety and stability of the patient.

In this design, an active BWS system which is composed of an electric linear actuator, a mechanical support, and a passive spring is presented in Fig. 6. A custom made harness is used to provide a comfortable lifting. The linear actuator provides large force to lift the body, and the passive spring is connected with the harness to absorb the ground impact. A position control of the BWS can be implemented using the electric servo system. The vertical motion of the BWS system is driven by the linear actuator. Since the stroke of the mechanical slider is 50 cm, the height of the BWS

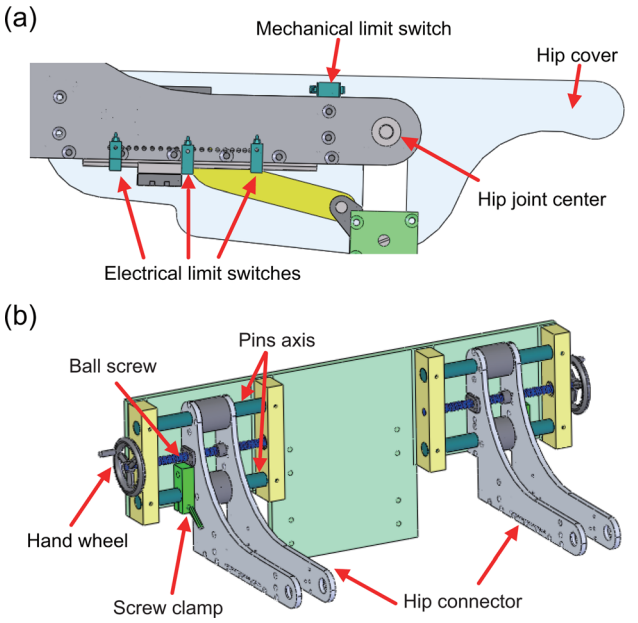

Fig. 8 (*a*) The limit switches in trunk segment and (*b*) the width adjustable device designed to adjust the distance between two orthoses

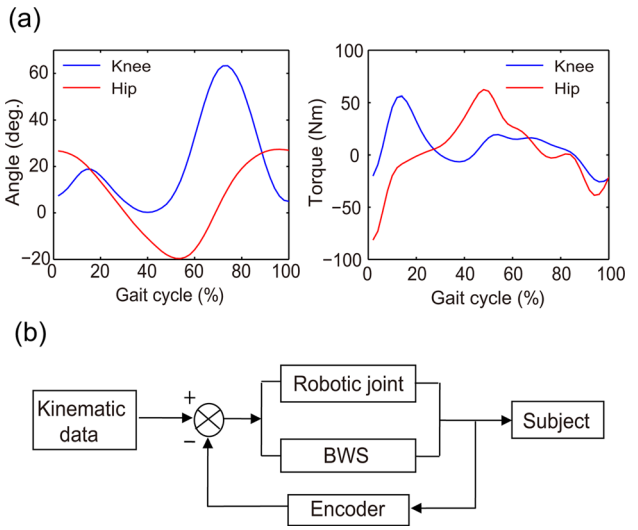

Fig. 9 (*a*) The gait angle and required torque on hip and knee joints, and (*b*) the flow diagram of the position control

system can be adjusted to satisfy patients with different heights (from 150 cm to 190 cm). A mobile base is motorized with two differential wheels to assist the walking and turning. Its speed is programmed according to the walking speed of the subject.

3.3 Sensors and Safety Devices. As shown in Fig. 7, a pressure sensor, which is composed of two airbags wrapped to the human leg, was developed to measure the interaction force between the human body and the robot [17,18]. During each measurement, both the pressure sensor and human leg are bound to the exoskeleton. Air is pumped into the bag, and the interaction force is directly calculated from the air pressure. It is beneficial to use this sensory device. For one thing, the compressed air in the bag produces active compliance, protecting patient from the stiff orthosis. For the other thing, the interaction force can be measured to realize force control of the exoskeleton. Additionally, surface

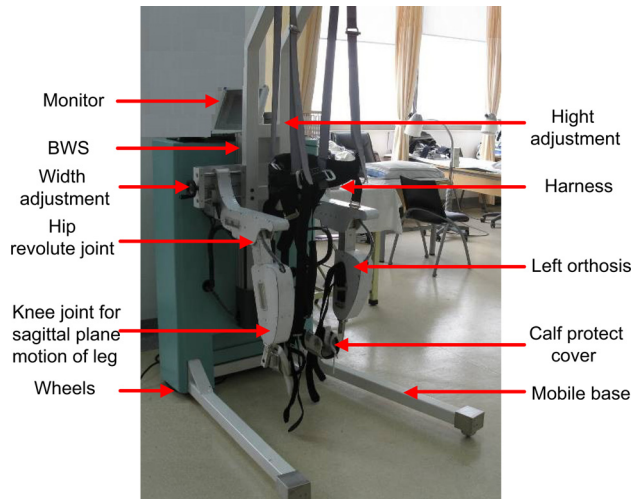

Fig. 10 Prototype of the MLLRE, its major components labeled

electromyography (sEMG) signals are collected to represent human muscle activation and evaluate rehabilitation performance.

Safety is another special concern for rehabilitation device. Several safety features are incorporated into this system. Mechanical limitation has been considered to prevent the joint angle from going beyond the physiological ROM. Limit switches (see Fig. 8(*a*)) were integrated into the orthosis to detect the position and restrict the stroke of the slider. An emergency stop circuit has been designed to cut off the power in case of any danger or if the subject feels uncomfortable using the device. Stop button was created such that a single push can stop the whole system.

As shown in Fig. 8(*b*), a width adjustable device is designed to connect the two robotic orthoses and the BWS system by axis pins. The distance between the two robotic orthoses is adjusted by rotating the hand wheel, on the purpose of fitting different weight patient. The location of the orthosis can be fixed by the screw clamp.

3.4 Electronics and Control System. AC servo motor (MINAS A5-series, Panasonic Industrial Devices Co., Ltd., Japan) is used in this system. This motor can operate in position or torque mode for rehabilitation. In addition, a synchronous belt drive is utilized to transmit the motor force into the ball screw, the transmission ratio of the belt drive for hip and knee is set to 1:1 and 11:18, respectively. Based on the normal kinematic gait data from CGA, the required joint torque is calculated in Fig. 9(*a*). The peak torque on hip and knee is $82\text{N}\cdot\text{m}$ and $62\text{N}\cdot\text{m}$. We computer the required motor torque on the hip and knee as $0.85\text{N}\cdot\text{m}$ and $0.42\text{N}\cdot\text{m}$, respectively. The motor power for hip and knee is selected as 400 W and 200 W, and the rated torque is $1.3\text{N}\cdot\text{m}$ and $0.64\text{N}\cdot\text{m}$, respectively. The robot can provide 150% assistance for normal gait walking (75 kg weight), thus it can meet large weight subject.

The heart of the robot system is a motion control card (GUC-800-TPV-M02-L2, Googol Technology Ltd., HK), which is an embedded controller consisting of both PC function and motion control function. In addition, the I/O interfaces are integrated to obtain the digital signal from limit switches. The flow chart of the position control for the robot is shown in Fig. 9(*b*). Kinematic data from the CGA are used as the desired trajectory. During each trial, training commands ordered by the therapist are sent to the control system.

4 Performance Evaluation

A prototype of the MLLRE has been implemented (see in Fig. 10). Before the clinical trial, the performance evaluation has

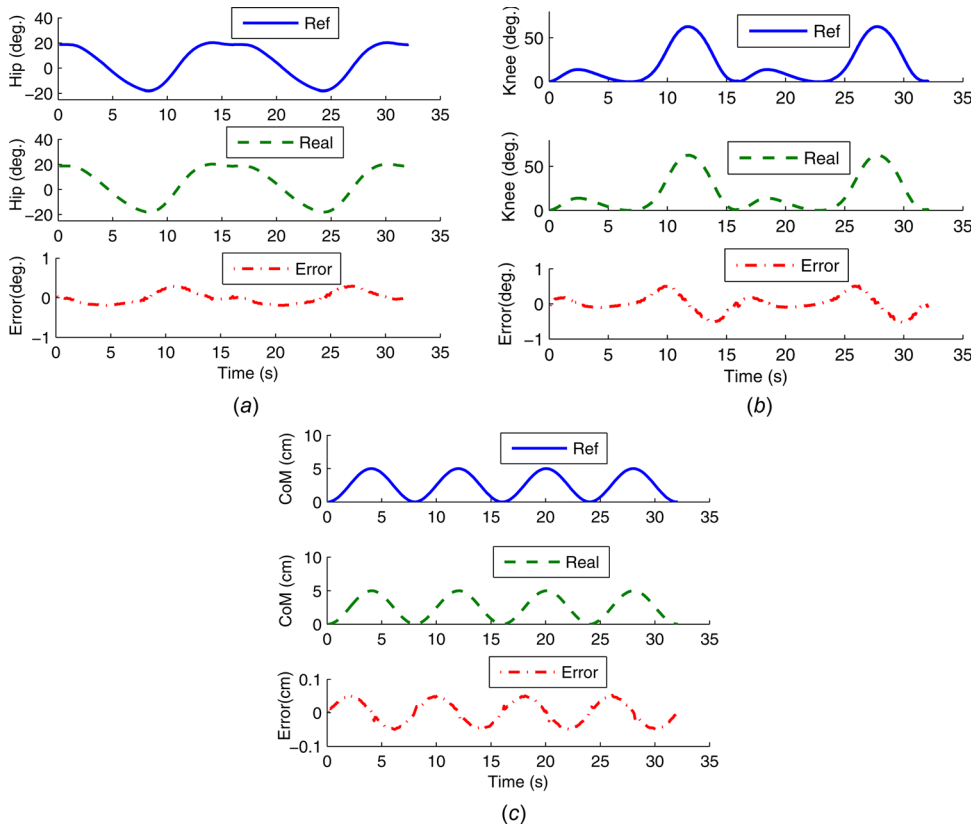

Fig. 11 Experiments with two gait cycles on a healthy subject, (solid line and dotted line represent the reference and real angles), (*a*) hip joint tracking, (*b*) knee joint tracking, and (*c*) COM tracking

been carried out on a healthy subject (age 28 years, body mass 70 kg). The control system is operating in the position mode. Figures 11(*a*) and 11(*b*) show the tracking experimental results with two gait cycles. The reference angle for hip and knee ranges from –20 deg to 20 deg and 0 deg to 62 deg, respectively. Gait cycle time was set to 16 s. It is illustrated that the tracking error in each joint is lower than 1 deg. The subject reported comfortable walking with the assistance of the robot. Figure 11(*c*) shows that the COM tracking error is lower than 0.1 cm. BWS system provides sufficient force to lift human body.

5 Conclusion and Future Work

This technical brief proposed a useful compact over-ground robotic exoskeleton which integrated two robotic orthoses with an active BWS device and a mobile base. We have implemented the position tracking which can help the patient passively walking under the support of the robot. This passive training is well suitable for patients who are in the early phase of rehabilitation. However, with regard to long term gait rehabilitation, exoskeleton should support patients only as much as needed (assist as needed) and stimulate them to produce maximal voluntary efforts, which means the patient should actively participate in the training process [19]. Force-based impedance control encourages patient self-movement, resisting the deviation from the reference trajectory. Some attempts have been done to integrate the impedance control into the rehabilitation strategy [9,10,19]. Based on the pressure sensor, the adaptive impedance-based assistance strategy will be investigated in the next step. Clinical trials for patients will be planned to investigate the performance of the over-ground training with this mobile exoskeleton in the future.

Acknowledgment

This work was supported by the National Basic Research Program of China (2011CB013203), the National Natural Science Foundation of China (61375098/61075101/60643002), the Science and Technology Intercrossing Research Foundation of Shanghai Jiao Tong University (LG2011ZD106), Dr. Zhao Guo was also supported by the Postdoctoral Science Foundation of China (2012M520887).

References

[1] Marchal-Crespo, L., and Reinkensmeyer, D. J., 2009, "Review of Control Strategies for Robotic Movement Training After Neurologic Injury," J. Neuroeng. Rehabil., **6**(1), p. 20.
[2] Cai, L. L., Fong, A. J., Otoshi, C. K., Liang, Y. Q., Burdick, J. W., Roy, R. R., and Edgerton, V. R., 2006, "Implications of Assist-as-Needed Robotic Step Training After a Complete Spinal Cord Injury on Intrinsic Strategies of Motor Learning," J. Neurosci., **26**(41), pp. 10564–10568.
[3] Dollar, A. M., and Herr, H., 2008, "Lower Extremity Exoskeletons and Active Orthoses: Challenges and State-of-the-Art," IEEE Trans. Rob., **24**(1), pp. 144–158.
[4] Strausser, K. A., and Kazerooni, H., 2011, "The Development and Testing of a Human Machine Interface for a Mobile Medical Exoskeleton," IEEE/RSJ International Conference on Intelligent Robots and Systems (IROS'11), San Francisco, CA, September 25–30, pp. 4911–4916.
[5] Esquenazi, A., Talaty, M., Packel, A., and Saulino, M., 2012, "The ReWalk Powered Exoskeleton to Restore Ambulatory Function to Individuals With Thoracic-Level Motor-Complete Spinal Cord Injury," Am. J. Phys. Med. Rehabil., **91**(11), pp. 911–921.
[6] Quintero, H. A., Farris, R. J., and Goldfarb, M., 2012, "A Method for the Autonomous Control of Lower Limb Exoskeletons for Persons With Paraplegia," ASME J. Med. Devices, **6**(4), p. 041003.
[7] Hesse, S., 2008, "Treadmill Training With Partial Body Weight Support After Stroke: A Review," NeuroRehabilitation, **23**(1), pp. 55–65.
[8] Riener, R., Lunenburger, L., Jezernik, S., Anderschitz, M., Colombo, G., and Dietz, V., 2005, "Patient-Cooperative Strategies for Robot-Aided Treadmill Training: First Experimental Results," IEEE Trans. Neural Syst. Rehabil. Eng., **13**(3), pp. 380–394.
[9] Veneman, J. F., Kruidhof, R., Hekman, E. E. G., Ekkelenkamp, R., Asseldonk, E. H. F. V., and van der Kooij, H., 2007, "Design and Evaluation of the LOPES Exoskeleton Robot for Interactive Gait Rehabilitation," IEEE Trans. Neural Syst. Rehabil. Eng., **15**(3), pp. 379–386.
[10] Banala, S. K., Kim, S. H., Agrawal, S. K., and Scholz, J. P., 2009, "Robot Assisted Gait Training With Active Leg Exoskeleton (ALEX)," IEEE Trans. Neural Syst. Rehabil. Eng., **17**(1), pp. 2–8.
[11] Stauffer, Y., Allemand, Y., Bouri, M., Fournier, J., Clavel, R., Metrailler, P., Brodard, R., and Reynard, F., 2009, "The WalkTrainer–A New Generation of Walking Reeducation Device Combining Orthoses and Muscle Stimulation," IEEE Trans. Neural Syst. Rehabil. Eng., **17**(1), pp. 38–45.
[12] Wang, P., Low, K. H., Tow, A., and Lim, P. H., 2011, "Initial System Evaluation of an Overground Rehabilitation Gait Training Robot (NaTUre-gaits)," Adv. Rob., **25**(15), pp. 1927–1948.
[13] Patton, J., Brown, D. A., Peshkin, M., Santos-Munne, J. J., Makhlin, A., Lewis, E., Colgate, J. E., and Schwandt, D., 2008, "KineAssist: Design and Development of a Robotic Overground Gait and Balance Therapy Device," Top Stroke Rehabil., **15**(2), pp. 131–139.
[14] Perry, J., and Davids, J. R., 1992, "Gait Analysis: Normal and Pathological Function," J. Pediatr. Orthop., **12**(6), p. 815.
[15] Saini, M., Kerrigan, D. C., Thirunarayan, M. A., and Duff-Raffaele, M., 1998, "The Vertical Displacement of the Center of Mass During Walking: A Comparison of Four Measurement Methods," ASME J. Biomech. Eng., **120**(1), pp. 133–139.
[16] Jezernik, S., Colombo, G., and Morari, M., 2004, "Automatic Gait-Pattern Adaptation Algorithms for Rehabilitation With a 4-DOF Robotic Orthosis," IEEE Rob. Autom. Mag., **20**(3), pp. 574–582.
[17] Yin, Y. H., Fan, Y. J., and Xu, L. D., 2012, "EMG and EPP-Integrated Human-Machine Interface Between the Paralyzed and Rehabilitation Exoskeleton," IEEE Trans. Inf. Technol. Biomed., **16**(4), pp. 542–549.
[18] Guo, Z., Fan, Y. J., Zhang, J. J., Yu, H., and Yin, Y. H., 2012, "A New 4M Model-Based Human-Machine Interface for Lower Extremity Exoskeleton Robot," 5th International Conference on Intelligent Robotics and Applications (ICIRA'12), Montreal, QC, Canada, October 3–5, pp. 545–554.
[19] Duschau-Wicke, A., von Zitzewitz, J., Caprez, A., Lunenburger, L., and Riener, R., 2010, "Path Control: A Method for Patient-Cooperative Robot-Aided Gait Rehabilitation," IEEE Trans. Neural Syst. Rehabil. Eng., **18**(1), pp. 38–48.